Available online at www.sciencedirect.com

ScienceDirect

Mendeleev Commun., 2024, **34**, 543–546

Mendeleev Communications

6-Phenyl-1,5-diazabicyclo[3.1.0]hexane: structure variations going from gas to crystal phase

Ilya I. Marochkin,[a] Pavel Yu. Sharanov,[a] Vladimir V. Kuznetsov,[b] Igor F. Shishkov*[a] and Yulia V. Novakovskaya[a]

[a] *Department of Chemistry, M. V. Lomonosov Moscow State University, 119991 Moscow, Russian Federation. E-mail: igormg@mail.ru*

[b] *N. D. Zelinsky Institute of Organic Chemistry, Russian Academy of Sciences, 119991 Moscow, Russian Federation*

DOI: 10.1016/j.mencom.2024.06.024

Based on gas electron diffraction experiments supported by quantum chemical simulations, the molecular structure of 6-phenyl-1,5-diazabicyclo[3.1.0]hexane (PhDBH) in the gas phase was determined, which is characterized by the puckering motion of the five-membered ring typical of bicyclo[3.1.0]-hexanes. It was found that the previously determined crystal packing is accompanied by a certain torsional twisting of the molecule, requiring activation energy. Based on the simulations of PhDBH clusters, it was shown that the energy is compensated by intermolecular interactions.

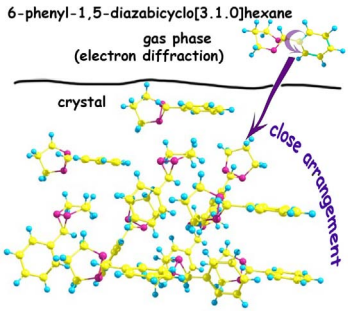

Keywords: gas electron diffraction, 1,5-diazabicyclo[3.1.0]hexane, molecular structure, cluster structures, BSSE correction.

The structures of diaziridines (diazacyclopropanes) are predetermined primarily by a three-membered nitrogen-containing ring with a certain amount of strain energy. Compared to monocycles, bicyclic systems usually have a fairly large strain energy.[1,2] Their relatively high positive enthalpies of formation make them candidates for high-energy density materials.[3,4] At the same time, the ignition characteristics of 1,5-diazabicyclohexane derivatives and the values of their half lethal doses, determined in toxicity studies, classify them as low-toxic hypergolic propellants.[5] From this point of view, diaziridine compounds can be considered very promising, and data on their reactivity, in particular under microwave (MW) irradiation conditions, are widely presented in the literature.[6]

The molecular geometries of several 1,5-diazabicyclohexane derivatives in the gas phase were studied by gas electron diffraction (GED).[7–13] The crystal structures of some of them were also determined by single-crystal X-ray diffraction (XRD).[14–16] In this work, we analyze the conformational behavior and molecular structure parameters of 6-phenyl-1,5-diazabicyclo[3.1.0]hexane (PhDBH) in the gas phase[†] in comparison with the known crystal structure determined by XRD experiment.[17]

Thermodynamic data for PhDBH, the first diaziridine for which the experimental enthalpy of crystal formation was obtained by bomb calorimetry, are reported.[3] It is noteworthy that the mechanism of thermal isomerization of PhDBH to 1-benzyl-4,5-dihydro-1*H*-pyrazole is described in a solution environment [DFT/B3LYP/6-31+G(d,p), PCM].[18,19] The rate constant of the thermal isomerization reaction of PhDBH ($k_1^{363} = 3.5 \times 10^{-5}$ s^{-1}) and the corresponding experimental Gibbs activation energy (33.9 kcal mol^{-1})[19] suggest that isomerization should not affect the results of the GED experiment, since the total time for heating the specimen and recording diffraction patterns does not exceed an hour.

Some information about the conformational landscape of PhDBH can be found in the published work,[19] where simulations were carried out at the DFT-B3LYP/6-31+G(d,p) level. Boat and chair conformations were identified, differing in the configuration of the 1,5-diazabicyclo[3.1.0]hexane (DBH) fragment. In the case of the chair conformation, it was found that both *exo*- and *endo*-orientation of the phenyl group are possible (Figure 1). In that work, the conformer with the twist configuration of the DBH fragment was quite reasonably not considered, since in the case of unsubstituted DBH, as a result of simulations at the MP2/6-31G(d,p) level it was found[7] that the twist conformer has a high relative Gibbs energy (47.9 kcal mol^{-1}) with a substantially elongated N–N bond (1.581 Å).

Taking these data into account, we analyzed the local domains of the molecular PES at the DFT and MP2 levels.[†] The aforementioned certain flexibility of the DBH fragment of the molecule actually predetermines the coexistence of its two

[†] GED experiment conditions are listed in Table S1 (see Online Supplementary Materials). Initial processing of the electron diffraction patterns was carried out by converting the optical density of the scanned images into total intensities $I(s)$ using the UNEX program[20] (Table S2). Vibmodule software[21] was used to calculate vibration amplitudes (u_{ij}) and internuclear distance corrections ($r_{ij,h1} - r_{ij,a}$) and ($r_{ij,e} - r_{ij,a}$) based on harmonic and cubic force fields computed within the second order Møller–Plesset (MP2) perturbation theory with the Dunning correlation-consistent cc-pVTZ basis set (Table S3).

Most of the quantum chemical calculations, including the search for stable conformers and transition state structures of a single PhDBH molecule, as well as force field calculations for the identified configurations, were carried out using the Gaussian 03 program.[22] The correspondence of the structures of all putative conformers to the minima of adiabatic potential energy was confirmed by the absence of imaginary vibrational frequencies.

Calculations of cluster structures were also carried out with the Firefly program[23] at the DFT level with the B3LYP hybrid exchange-correlation functional[24,25] and the 6-31G(d,p) basis set. The results were visualized using Chemcraft.[26] To predict the crystal density, the DFT method with the B3PW91 functional with non-local correlation[27] was used.

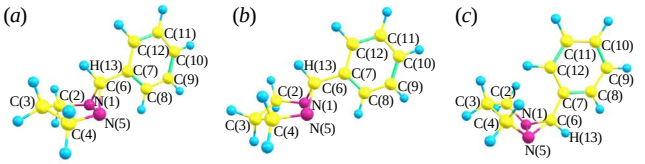

Figure 1 Conformers of the PhDBH molecule: (*a*) boat, (*b*) *exo*-chair and (*c*) *endo*-chair.

conformations. In total, three PhDBH conformers were found, all with C_s symmetry due to the location of the phenyl ring in the mirror plane of the DBH fragment. The MP2/cc-pVTZ estimates indicate that the *exo*-chair conformer has a 3.4 kcal mol^{-1} lower relative ZPE-corrected energy. At the same time, the search for the transition state between the chair and boat conformers, carried out at the DFT-B3PW91/6-31G(d,p) level, showed that the corresponding saddle point is located closer to the chair conformer than to the flat conformer: the N(1)–N(5)–C(4)–C(3) dihedral angle in the diazabicyclo[3.1.0]hexane fragment is 12.1°. Its potential energy is about 3.8 kcal mol^{-1} higher than that of the boat conformer, which is only slightly higher than that of the *exo*-chair conformer. The latter fact means that, even when formed under certain conditions, this chair conformer must be a short-lived species due to the very low barrier separating it from the more stable boat conformer. It was calculated (Table S4) that zero-point energy corrections only slightly change the relative energies of the conformers, and thermal increments consistent with the GED experiment do not make the existence and interconversions of the isomers more likely. This means that the interpretation of experimental data can be based solely on the initial approximation corresponding to the boat conformer only.

The molecular GED model of the title compound was based on 21 internuclear distances, 18 bond angles and 12 dihedral angles (see Online Supplementary Materials). The mean vibrational amplitudes were refined in seven groups according to the positions of the peaks of internuclear distances related to the characteristic ranges of the radial distribution curve $f(r)$, namely: 1.39–1.53, 2.37–2.51, 2.71–2.96, 3.71–3.77, 4.19–4.41, 4.73–4.87 and 5.02–6.47 Å. The best agreement between observed and theoretical molecular electron scattering intensities for PhDBH was achieved with a moderate disagreement factor R_f of 5.9%. There is good overall agreement between the final GED structure parameters and those predicted at both the MP2 and DFT levels (Table 1). The resulting differences fall within the confidential intervals.

To date, various bicyclo[3.1.0]hexane molecules and nitrogen-containing DBHs have been widely studied by GED and MW spectroscopy (Figure S2, see Online Supplementary Materials). The presence of a strained bicyclic system makes it possible to distinguish their structures with their inherent puckering motion of five-membered rings. As follows from the geometric parameters of the DBH fragment of these molecules (Table S6), they are all quite close. No significant deviations can be identified. The length of the C–N bond in the diaziridine fragment is shorter by 0.026 Å compared to the adjacent C–N bond, which, however, may not be statistically significant due to the magnitude of the specified uncertainty. Interestingly, the C–C(H_2)–C bond angle is closer to those in unsubstituted DBH and sabinene. At the same time, the effect of the phenyl substituent is manifested in the N–C_{diaz}–C_{Ph} angle with a difference of 2.9°.

The parameters commonly used in relation to the deformation dynamics of the PhDBH molecule are the puckering angles for the five-membered ring (Table S6). As follows from the data in Table S6, the β angle ranges from 63.0° to 74.6° regardless of the nature of the substituent, while the α angle is more sensitive to the presence of substituents, being largest (38°) in the unsubstituted ring and smallest (1.2°) in the presence of two methyl groups in the three-membered ring. Here the phenyl ring has almost the same conformational effect as the methyl group (24.4° *vs.* 26.2°, respectively). However, unlike the methyl group, the phenyl group is additionally characterized by the possibility of internal rotation relative to the bicyclic fragment.

Table 1 Selected geometric parameters of the PhDBH structure refined using data from the GED experiment, compared with the initial theoretical estimates at the MP2/cc-pVTZ and DFT-B3LYP/cc-pVTZ levels and the XRD crystal structure.

Parameter	GED[a]	MP2/ cc-pVTZ	B3LYP/ cc-pVTZ	XRD[b]
	Internuclear distances r_e/Å			Bond lengths/Å
C(6)–N(1)	1.444(21)	1.456	1.454	1.459(4)
N(1)–N(5)	1.506[c]	1.506	1.495	1.494(4)
N(1)–C(2)	1.470(24)	1.477	1.478	1.478(5)
C(2)–C(3)	1.530(12)	1.531	1.538	1.526(6)
C(6)–H(13)	1.087[c]	1.087	1.087	0.980(3)
C(6)–C(7)	1.476(12)	1.477	1.486	1.487(4)
$(C_{cycl}–H)_{av}$	1.089[c]	1.089	1.090	0.980(3)
$C_{Ph}–C_{Ph}$	1.388(4)	1.394	1.391	1.392(4)
$(C_{Ph}–H)_{av}$	1.082[c]	1.082	1.082	
	Bond angles/deg			
N(1)–N(5)–C(4)	108.5(14)	107.2	107.8	107.6(3)
N(1)–C(6)–H(13)	117.5(12)	116.9	116.9	115.9(3)
N(1)–C(6)–C(7)	117.8(40)	117.9	119.0	118.0(3)
N(5)–C(4)–H	109.5(14)	108.9	109.4	110.1(4)
C(6)–C_{Ph}–C_{Ph}	120.4(14)	120.1	120.8	121.5(3)
$(C_{Ph}–C_{Ph}–C_{Ph})_{av}$	120.3(14)	119.8	120.1	
	Dihedral angles/deg			
C(6)–N(1)–N(5)–C(4)	105.4[c]	105.4	106.9	105.7(3)
N(5)–C(2)–C(4)–C(3)	155.6(60)	153.5	156.2	153.9(4)
C(12)–C(7)–C(6)–H(13)	0.0[c]	0.0	0.0	17.1(4)
	Total disagreement factor R_f[d] (%)			
	5.9			

[a] Errors are the standard deviation of the least squares refinement: $3\sigma_{LS}$ for bond lengths and $2\sigma_{LS}$ for bond angles and dihedral angles. [b] Reference 17. [c] Fixed to theoretical value. [d] R_f is calculated as $\{\sum[sM^{exp}(s) - sM^{theor}(s)]^2\}/\{\sum[sM^{exp}(s)]^2\}^{1/2}$.

There is a clear difference between the structure of an individual molecule in the gas phase and the same molecule

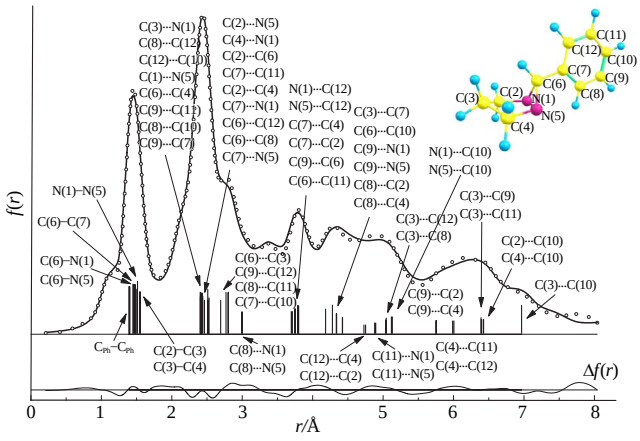

Figure 2 Experimental (open circles) and theoretical (solid line) radial distribution curves $f(r)$ and their difference curve $\Delta f(r)$ for the PhDBH molecule. Vertical bars show the distribution of intramolecular distances between heavy atoms. Atom numbering is shown in the inset.

embedded in a crystal lattice. Here, the torsion angle C_{Ph}–C_{Ph}–C–H [C(12)–C(7)–C(6)–H(13)] can be taken as a convenient parameter for considering the geometry of the molecule. When the molecule is in the gas phase, this angle is 0° due to its C_s symmetry and reaches 17.1(4)° when the molecule is in the crystalline phase. This means that in the crystal the geometry of the molecule is substantially distorted due to the rotation of the phenyl ring around the C(6)–C(7) bond.

Another interesting and spectacular geometric parameter of the molecule is the N–N distance, which increases from 1.506 Å in the boat conformer to 1.531 Å in the *exo*-chair conformer and decreases to 1.500 Å in the higher energy *endo*-chair conformer (B3LYP/cc-pVTZ). Although the chair conformers of PhDBH are unlikely to exist under the conditions considered (see above), the relative smoothness of the neighboring potential energy cross sections makes certain variations in the N–N distance quite possible, which is important in view of its shortening when molecules pack into a crystal. It is worth noting that the chair conformations of some DBHs can be favorable when the puckered C(3) atom in the five-membered cycle bears alkyl substituents. This can cause steric hindrance in the case of the boat conformer and reduce its stability, which leads in the case of 3,3-dimethyl-1,5-diazabicyclo[3.1.0]hexane to the predominance of the chair conformer in the amount of 68(8)% at a temperature of 330 K.[28]

The permissible ranges of spatial parameters predetermine changes in structure during the packing of molecules in crystals and are reflected in specific space groups. As found in previous XRD studies,[14–17] PhDBH and related compounds substituted at position 6 with 4-RC_6H_4 (R = OMe, Br and Cl) crystallize primarily in orthorhombic lattices (Table S7). A monoclinic space group was identified in the case of 3,3-dimethyl-1,5-diazabicyclo[3.1.0]hexane derivatives and compounds of the bicyclic DBH series. Since the compactness of the packing predetermines the density, the latter is a good visual indicator. The density of PhDBH is 1.207 g cm^{-3} (mp 93 °C), which is higher than that of unsubstituted DBH of 1.03 g cm^{-3} (mp −9.5 °C)[4] and comparable to the densities of known related compounds, despite the presence of heavy atoms in most of them.

The relatively high density even in the absence of bromine, chlorine or oxygen substitution on the phenyl ring, as well as the obvious correlation between the density and molecular weight of all PhDBHs, generate interest in their crystal packing from both theoretical and practical points of view. In addition, three different fragments of the molecule, namely the aromatic phenyl ring, the sequence of saturated methylene groups and the diaza bridge between them, undergo a very noticeable twist upon aggregation, that is, the phenyl ring tilts to the plane normal to the diaza bridge by about 17°. The corresponding energy difference is not large: the transformation in the single molecule requires an activation energy of approximately 0.25 to 0.30 kcal mol^{-1} [estimated at the MP2/6-31G(d,p) and MP2/cc-pVTZ levels], which correlates with a low frequency of such internal rotation, approximately 35 to 43 cm^{-1}. However, this energy must be transferred to the molecule, which would be natural if the transition occurred upon heating. In the case of the PhDBH molecule, the transformation is reverse: upon cooling, it crystallizes in a distorted configuration. What is the source of perturbation and subsequent stabilization of distorted molecules and how does this correlate with the nature of the packing?

Regarding the crystal packing density of energy-rich substances consisting of C, H, N and O atoms, Politzer noted that the commonly used M/V_m estimation of the neutral crystal density, where M is the molecular mass (g per molecule) and V_m is the volume of an isolated molecule in the gas phase (cm^3 per molecule), may not be accurate.[29] An attempt to relate the density of neutral molecular crystals to molecular electrostatic potential descriptors ($\nu\sigma^2_{tot}$), computed on 0.001 a.u. molecular surfaces, and coefficients (α, β and γ) found by the least squares fitting of the available data has led to an approximation in the form[29,30]

$$\rho = \alpha_1(M/V_m) + \beta_1(\nu\sigma^2_{tot}) + \gamma_1. \quad (1)$$

The crystal density of PhDBH, estimated from the M/V_m ratio at the DFT-B3LYP and MP2 levels of theory, ranges from 1.217 to 1.243 g cm^{-3} (Table S8), exceeding ρ_{exp} = 1.207 g cm^{-3} by less than 0.05 g cm^{-3}, which, according to Kim's criteria,[31] can be classified as an 'informative' prediction. It is worth noting that the estimates obtained with the same cc-pVTZ basis set nearly coincided and amounted to *ca.* 1.23 g cm^{-3}. When equation (1) was used with either the Politzer or Rice parameter set, the estimates were 1.242 and 1.215 g cm^{-3}, respectively, if taken to exactly the same approximations as those used to parameterize the equation. It is likely that the first value, as well as the straightforward estimates given above, overrates the density, while the second already seems reasonable. It is close to what is considered an 'excellent' estimate, where the error does not exceed 0.03 g cm^{-3}.

To clarify the strength of interactions that can control distortions and compact packing of molecules in crystals, PhDBH molecular aggregates containing up to seven molecules were identified and cut off. These configurations served as initial approximations of cluster structures, which were then optimized at the B3LYP/6-31G(d,p) level and their correspondence to local minima of the adiabatic potential was confirmed by the absence of imaginary vibrational frequencies.

The boat configuration for the DBH fragment was predicted to be the only conformation stable in both the gas and crystalline phases. It was conserved in all molecules of all clusters considered. At the same time, the C_{Ph}–C_{Ph}–C–H dihedral angles, equal to *ca.* 17° in the crystal lattice and 0° in the gas phase, fall in the range from 0.0° to 18.4° for different molecules in clusters and approach zero for molecules with the smallest number of neighbors. This result shows that it is the interactions between molecules that cause distortion of the molecular structure, and the corresponding forces depend on the mutual arrangement of the molecules. It is noteworthy that in the considered clusters the C_{Ph}–C_{Ph}–C–H dihedral angle is close to 17° mainly for one molecule, while the conformations of the remaining molecules are closer to the conformation in the gas phase (Table S9). This is a molecule that is subject to a superposition of neighboring effects and that most closely resembles a molecule in a crystal structure.

Analysis of vibrational frequencies in an individual PhDBH molecule showed that vibration with a frequency from 34 to 43 cm^{-1} (according to MP2 estimates) corresponds to almost pure internal rotation around the C_{diaz}–C_{Ph} bond, and the contribution of the corresponding oscillations of the C_{Ph}–C_{Ph}–C–H dihedral angle to vibrational energy was 86%. Vibration energy analysis of the clusters, carried out at the B3LYP/6-31G(d,p) level, revealed changes in both the frequencies and the composition of the related vibrational coordinates. For example, in a heptamer these oscillations have frequencies ranging from 35 to 86 cm^{-1} with varying energy contributions of individual molecules from 10 to 36% depending on the degree of coupling between these internal rotations of different molecules and the restricted rotational vibrations of neighboring molecules as a whole. Thus, the coupling strongly hampers internal rotations; and in a molecule with the C_{Ph}–C_{Ph}–C–H angle closest to that in the crystal structure, the frequency is nearly twice as high as in an individual gas phase molecule, about 67 cm^{-1}. This means that crystal packing is accompanied by an increase in the rigidity (with respect to internal rotation) of the molecules.

The corresponding interaction energy can be estimated tentatively by considering the same molecular aggregates with a relative arrangement of molecules similar to that in the crystal lattice. The character of bonding can be judged from the adiabatic and vertical dissociation energies. Both characteristics were evaluated taking into account the basis set superposition error (BSSE) in the conventional counterpoise variant. For example, when three PhDBH molecules are arranged as in a crystal lattice, the vertical dissociation energy of the aggregate is 1.0 kcal mol^{-1}. When optimizing the configuration of the entire aggregate, the vertical dissociation energy increases to 1.6 kcal mol^{-1}, while the adiabatic one is equal to 1.4 kcal mol^{-1} (Table S10), which shows that interactions within bimolecular pairs are about 0.4 kcal mol^{-1} on the average. In a heptamer, the dissociation energy is already 7.8–8.4 kcal mol^{-1} depending on whether the relaxation of monomers is taken into account or not, which amounts to about 0.6 kcal mol^{-1} per intermolecular contact. As can be seen, the value increases with the number of nearest neighbors of the molecules; but if the energy is normalized by the number of molecules, then it will be greatest when the total twisting distortion of the molecules is least. This means that the interaction is stronger, the closer the molecular configurations are to those typical for the gas phase. At the same time, even when all the molecules are torsionally twisted, the energy of their interaction is sufficient to compensate for the required distortion and make them more closely packed.

Thus, based on the experimental electron diffraction data and quantum chemical simulations, the structure of the PhDBH molecule in the gas phase was determined and found to differ from the configuration typical for the packing of a crystal lattice. The key difference is that in the gas phase the bisector of the N–C–N angle in the diaza fragment lies in the plane of the phenyl ring, and when packed into a crystal lattice, the plane of the phenyl ring is tilted by *ca.* 17º. At the same time, only the boat conformation of the DBH fragment was observed in both phases. As follows from the simulation results, the required internal rotation of the phenyl ring with respect to the diaza bicycle in molecules can be promoted by favorable intermolecular interactions, which, apparently, are also responsible for the relatively compact arrangement of the molecules, so that the predicted packing density tends to be higher than the previously suggested XRD estimate.

I.I.M., P.Yu.Sh., I.F.Sh. and Y.V.N. acknowledge that this work was carried out within the framework of the state assignment of the Russian Federation ‘Molecular and supramolecular organization of compounds, hybrid and functional materials’ (contract no. 121031300090-2).

Online Supplementary Materials

Supplementary data associated with this article can be found in the online version at doi: 10.1016/j.mencom.2024.06.024.

References

1 P. R. Rablen, *Chemistry*, 2020, **2**, 347.
2 S.-J. Chang, D. McNally, S. Shary-Tehrany, S. M. J. Hickey and R. H. Boyd, *J. Am. Chem. Soc.*, 1970, **92**, 3109.
3 V. A. Lukyanova, V. V. Kuznetsov, N. M. Konstantinova, A. S. Dmitrenok, M. P. Kosaya, O. V. Dorofeeva and A. I. Druzhinina, *Phys. Chem. Chem. Phys.*, 2023, **25**, 25289.
4 X. Zhang, L. Shen, Y. Luo, R. Jiang, H. Sun, J. Liu, T. Fang, H. Fan and Z. Liu, *Ind. Eng. Chem. Res.*, 2017, **56**, 2883.
5 X. Zhang, L. Shen, R. Jiang, H. Sun, T. Fang, Z. Liu, J. Liu and H. Fan, *Propellants, Explos., Pyrotech.*, 2017, **42**, 477.
6 A. P. Molchanov, M. M. Efremova, M. A. Kryukova and M. A. Kuznetsov, *Beilstein J. Org. Chem.*, 2020, **16**, 2679.
7 Y. V. Vishnevskiy, N. Vogt, J. Vogt, A. N. Rykov, V. V. Kuznetsov, N. N. Makhova and L. V. Vilkov, *J. Phys. Chem. A*, 2008, **112**, 5243.
8 E. G. Atavin, A. V. Golubinskii, M. V. Popik, V. V. Kuznetsov, N. N. Makhova and L. V. Vilkov, *J. Struct. Chem.*, 2003, **44**, 779 (*Zh. Strukt. Khim.*, 2003, **44**, 851).
9 L. S. Khaikin, G. G. Ageev, A. N. Rykov, O. E. Grikina, I. F. Shishkov, I. V. Kochikov, V. V. Kuznetsov, N. N. Makhova, S. S. Bukalov and L. A. Leites, *Phys. Chem. Chem. Phys.*, 2020, **22**, 22477.
10 G. G. Ageev, A. N. Rykov, O. E. Grikina, I. F. Shishkov, I. V. Kochikov, V. V. Kuznetsov, N. N. Makhova and S. S. Bukalov, *Struct. Chem.*, 2022, **33**, 113.
11 I. I. Marochkin, V. V. Kuznetsov, A. N. Rykov, N. N. Makhova and I. F. Shishkov, *Struct. Chem.*, 2019, **30**, 457.
12 I. I. Marochkin, V. V. Kuznetsov, Z. Li, A. N. Rykov, N. N. Makhova and I. F. Shishkov, *J. Mol. Struct.*, 2021, **1225**, 129066.
13 G. G. Ageev, V. V. Kuznetsov, A. N. Rykov and I. F. Shishkov, *Mendeleev Commun.*, 2023, **33**, 515.
14 V. V. Kuznetsov, S. A. Kutepov, N. N. Makhova, K. A. Lyssenko and D. E. Dmitriev, *Russ. Chem. Bull.*, 2003, **52**, 665 (*Izv. Akad. Nauk, Ser. Khim.*, 2003, 638).
15 V. V. Kuznetsov, D. V. Khakimov, A. S. Dmitrenok and A. S. Goloveshkin, *J. Mol. Struct.*, 2022, **1269**, 133856.
16 I. N. Kolesnikova, V. V. Kuznetsov, A. S. Goloveshkin, N. A. Chegodaev, N. N. Makhova and I. F. Shishkov, *Struct. Chem.*, 2021, **32**, 2303.
17 A. P. Molchanov, D. I. Sipkin, Yu. B. Koptelov, J. Kopf and R. R. Kostikov, *Russ. J. Org. Chem.*, 2003, **39**, 1338 (*Zh. Org. Khim.*, 2003, **39**, 1410).
18 A. P. Molchanov, D. I. Sipkin, Yu. B. Koptelov and R. R. Kostikov, *Russ. J. Org. Chem.*, 2001, **37**, 841 (*Zh. Org. Khim.*, 2001, **37**, 888).
19 T. A. Kornilova, R. R. Kostikov, A. F. Khlebnikov and I. G. Zenkevich, *J. Phys. Org. Chem.*, 2018, **31**, e3843.
20 [dataset] Y. V. Vishnevskiy, *UNEX*, version 1.6, 2023, https://unex.vishnevskiy.group/en/.
21 Y. V. Vishnevskiy and Y. A. Zhabanov, *J. Phys.: Conf. Ser.*, 2015, **633**, 012076.
22 M. J. Frisch, G. W. Trucks, H. B. Schlegel, G. E. Scuseria, M. A. Robb, J. R. Cheeseman, J. A. Montgomery, Jr., T. Vreven, K. N. Kudin, J. C. Burant, J. M. Millam, S. S. Iyengar, J. Tomasi, V. Barone, B. Mennucci, M. Cossi, G. Scalmani, N. Rega, G. A. Petersson, H. Nakatsuji, M. Hada, M. Ehara, K. Toyota, R. Fukuda, J. Hasegawa, M. Ishida, T. Nakajima, Y. Honda, O. Kitao, H. Nakai, M. Klene, X. Li, J. E. Knox, H. P. Hratchian, J. B. Cross, V. Bakken, C. Adamo, J. Jaramillo, R. Gomperts, R. E. Stratmann, O. Yazyev, A. J. Austin, R. Cammi, C. Pomelli, J. W. Ochterski, P. Y. Ayala, K. Morokuma, G. A. Voth, P. Salvador, J. J. Dannenberg, V. G. Zakrzewski, S. Dapprich, A. D. Daniels, M. C. Strain, O. Farkas, D. K. Malick, A. D. Rabuck, K. Raghavachari, J. B. Foresman, J. V. Ortiz, Q. Cui, A. G. Baboul, S. Clifford, J. Cioslowski, B. B. Stefanov, G. Liu, A. Liashenko, P. Piskorz, I. Komaromi, R. L. Martin, D. J. Fox, T. Keith, M. A. Al-Laham, C. Y. Peng, A. Nanayakkara, M. Challacombe, P. M. W. Gill, B. Johnson, W. Chen, M. W. Wong, C. Gonzalez and J. A. Pople, *Gaussian 03*, Gaussian, Inc., Wallingford, CT, 2004.
23 [dataset] A. A. Granovsky, *Firefly Computational Chemistry Program*, version 8, http://classic.chem.msu.su/gran/gamess/index.html.
24 C. Lee, W. Yang and R. G. Parr, *Phys. Rev. B.: Condens. Matter Mater. Phys.*, 1988, **37**, 785.
25 A. D. Becke, *J. Chem. Phys.*, 1993, **98**, 5648.
26 [dataset] *Chemcraft – Graphical Software for Visualization of Quantum Chemistry Computations*, version 1.8 (build 682), https://www.chemcraftprog.com.
27 A. D. Becke, *J. Chem. Phys.*, 1992, **97**, 9173.
28 Y. V. Vishnevskiy, J. Schwabedissen, A. N. Rykov, V. V. Kuznetsov and N. N. Makhova, *J. Phys. Chem. A*, 2015, **119**, 10871.
29 P. Politzer, J. Martinez, J. S. Murray, M. C. Concha and A. Toro-Labbé, *Mol. Phys.*, 2009, **107**, 2095.
30 B. M. Rice and E. F. C. Byrd, *J. Comput. Chem.*, 2013, **34**, 2146.
31 C. K. Kim, S. G. Cho, C. K. Kim, H.-Y. Park, H. Zhang and H. W. Lee, *J. Comput. Chem.*, 2008, **29**, 1818.

Received: 4th March 2024; Com. 24/7412